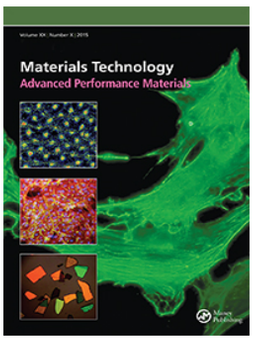

Taylor & Francis
Taylor & Francis Group

Materials Technology
Advanced Performance Materials

ISSN: 1066-7857 (Print) 1753-5557 (Online) Journal homepage: http://www.tandfonline.com/loi/ymte20

Effect of halloysite nanotubes loading on thermo-mechanical and morphological properties of polyurethane nanocomposites

T. S. Gaaz, A. B. Sulong, M. N. M. Ansari, A. A. H. Kadhum, A. A. Al-Amiery & M. S. H. Al-Furjan

To cite this article: T. S. Gaaz, A. B. Sulong, M. N. M. Ansari, A. A. H. Kadhum, A. A. Al-Amiery & M. S. H. Al-Furjan (2016): Effect of halloysite nanotubes loading on thermo-mechanical and morphological properties of polyurethane nanocomposites, Materials Technology, DOI: 10.1080/10667857.2016.1265278

To link to this article: http://dx.doi.org/10.1080/10667857.2016.1265278

Published online: 20 Dec 2016.

MATERIALS TECHNOLOGY, 2016
http://dx.doi.org/10.1080/10667857.2016.1265278

Taylor & Francis
Taylor & Francis Group

Effect of halloysite nanotubes loading on thermo-mechanical and morphological properties of polyurethane nanocomposites

T. S. Gaaz[a,e], A. B. Sulong[a], M. N. M. Ansari[b], A. A. H. Kadhum[c], A. A. Al-Amiery[c] and M. S. H. Al-Furjan[d]

[a]Faculty of Engineering & Built Environment, Department of Mechanical & Materials Engineering, Universiti Kebangsaan Malaysia, Bangi, Malaysia; [b]Center for Advanced Materials, College of Engineering, Universiti Tenaga Nasional, Kajang, Malaysia; [c]Faculty of Engineering & Built Environment, Department of Chemical & Process Engineering, Universiti Kebangsaan Malaysia, Bangi, Malaysia; [d]School of Mechanical Engineering, Hangzhou Dianzi University, Hangzhou, China; [e]Department of Machinery Equipment Engineering Techniques, Technical College Al-Musaib, Al-Furat Al-Awsat Technical University, Al-Musaib, Iraq

ABSTRACT

Halloysite-(0.1, 0.5.1.0, 1.5, 2.0 wt%) polyurethane (PU-HNT) nanocomposites were synthesised. Mechanical, thermal, water absorption and morphological properties of PU and its relevant PU-HNT nanocomposites were studied. Scanning electron microscope images of PU and PU-HNT-fractured surfaces show cracks and agglomeration at 1·0 wt.% HNT. The thermomechanical properties of the PU-HNT nanocomposites have improved up to 1·0 wt.% HNT; however, they were adversely affected by more HNT loading. Despite this reduction, the mechanical properties are still better than that of neat PU. The mechanical strength increased as HNT content was up to 1·0 wt.%. Tensile, flexural, and impact strength of the PU-HNT nanocomposite were found to be 11·78 MPa, 128·15 MPa, and 5·57 × 103 J mm^{-2}, respectively, at 1·0 wt.% HNT. Thermal studies showed that thermal stability and crystallisation temperature of the PU-HNT nanocomposite increased compared to that of PU. The loss modulus curves showed that pure PU crystallises at 126°C and at 129 for PU -0·1 wt.% of HNT. PU-TGA rises with increasing loading from 0·1 to 2·0 wt.%. The water absorption of the PU-HNT nanocomposite has shown moisture in PU-2·0 nanocomposite in 21-day treatment.

ARTICLE HISTORY
Received 6 May 2016
Accepted 18 November 2016

KEYWORDS
Halloysite nanotubes; nanocomposite; thermal stability; mechanical properties; polyurethane

Introduction

Polymers have recently caught attention due to their vast industrial and medical applications and the relatively inexpensive cost of fabrication and processing. Polyurethanes (PUs) are not different polymers from other polymers but, in addition, their principal chain structure is composed of rigid hard and flexible soft segments.[1] The hard and soft segments are characterised by a specific micro-phase structure which made PUs with high mechanical strength, good elasticity and abrasion resistance and controllable hardness. These properties play important roles in coatings, adhesives, foams, fibres, paints, elastomers and synthetic skin.[2,3] The drawback of the conventional PU products is that PU products contain a significant amount of organic solvents [4] and free isocyanate monomers.[5] In addition, the PU film which contains 50–70 wt.% renewable vegetable oil polyol could result in improving the thermo-physical and mechanical properties comparable to PUs from petroleum-based polyols.[6,7] The filler, halloysite nanotubes (HNTs), is a kind of aluminosilicate clays with hollow nanotubular structure [8] are naturally found in many countries such as China, America, Brazil, France and others. The chemical structure of HNTs is similar to kaolinite with only one difference which is related to the location of OH group. Traditionally, HNTs are used in manufacturing high-quality, a white-ware ceramic.[9] However, recently HNTs have been used as nanotemplates or nanoscale reaction vessels instead of CNTs [10] or boron nitride nanotubes (BNNTs).[8,11] In other recent application, HNTs were utilised as nanofillers polymers such as natural rubber, nitrile rubber and thermoplastic.[12] The overall applications of HNTs focus on reinforcing the host polymers to produce epoxy resin or natural rubber.[13–16] The nanocomposites, in many cases, exhibit remarkable improvements in mechanical,[17,18] thermal [19,20] and barrier [21,22] properties with a low loading of clay in the polymer matrix. The nanocomposite products are usually very important tools by providing a very simple approach to investigate complex confined system.[23,24] Despite the fact that HNTs has proven its function ability as a reinforcing agent for polymers, there are on-growing attempts to use HNT's counterpart, CNTs, as an excellent candidate with other

CONTACT T. S. Gaaz taysersumer@gmail.com; A. B. Sulong abubakar@ukm.edu.my Faculty of Engineering & Built Environment, Department of Mechanical & Materials Engineering, Universiti Kebangsaan Malaysia, Bangi, Malaysia

Table 1. Chemical compositions of HNT.

Chemical compositions	SiO_2	Al_2O_3	Fe_2O_3	MgO	TiO_2
Weight %	61·19	18·11	0·49	0·10	20·11

Table 2. Physical properties of HNT.

Typical analysis of natural HNT	
Chemistry	$Al_2Si_2O_5(OH)_4{\cdot}nH_2O$
d50(median particle size)	1·0 μ
Aspect ratio (L/D)	~15
Surface area (BET)	65 $m^2\ g^{-1}$
Specific gravity	2·54 g cm^{-3}
Refractive Index	1·54

materials for enforcement such as poly(3-hexylthiophene) (P3HT),[25] $Mg_{59.5}Cu_{22.9}Gd_{11}Ag_{6.6}$ bulk metallic glass [26] or as a substrate to perform epitaxial periodic crystallisation of polymer.[27]

The remarkable applications of PU are in the medical fields due to simple fabrication, bioflexibility, biostability and very good electrical insulation property. However, the remarkable applications are restrained by PU degrading which results in deep cracking, stiffening, erosion or the deterioration of mechanical properties such as tensile and flexural strength. Despite these drawbacks, the future of PU nanocomposites is very optimistic and the goal is always to produce soft and tough biomedical implants.[28,29] Additionally, improving HNT nanotubes without using it as fillers with other polymers has been recently investigated.[30] It was found that upon mixing amylose with HNT through a process called wrapping, amylose reacts with the outer surface of HNT which results in significant improvement of mechanical properties of HNT. The process was explained throughout the general practice where the ability of HNT-amylose is enhanced in absorbing metal ions.[31] In other biomedical applications, HNT is used for storing molecular hydrogen which helps in hydrocarbon processing and catalytic conversions. HNT has used also in the environmental sectors in manufacturing devices such as a diuretic drug transportation to remove hazardous species. For non-implant devices, HNT is used in drug transportation to remove hazardous species, sustained release of drugs, food additives, fragrances and antimicrobial agents. In implant devices, HNT has a variety of chemical interactions which yield better corrosion in breast cells and also used in biosensors.[31]

In continuation of previous studies [32–37] on nanomaterials and catalysts, herein we are reporting the synthesis and investigating a new composite suitable for mechanical and thermal applications. Mechanical and thermal characterisations were conducted such as tensile strength, % elongation, modulus, flexural strength and impact strength. Thermal properties include glass transition temperature, crystallisation temperature, melting temperature, storage modulus, loss modulus and the degradation temperature of the nanocomposites. This study also covers morphological properties and water absorption characteristics.

Experimental

Materials

PU was obtained from Global Innovations-Polycarbonates Bayer Material Science AG, D-51368 Leverkusen. HNT was supplied by Natural Nano, Inc., 832 Emerson Street Rochester, New York 14613. The chemical compositions and physical properties of HNTs are tabulated in Tables 1 and 2, respectively.

Sample preparation and experimental set-up

The sample preparation and the experimental procedure were conducted according to the flow chart shown in Figure 1. Five samples were prepared by loading HNT with PU at 0·1, 0·5, 1·0, 1·5 and 2·0 wt.%. Scanning electron microscope (SEM) along with other devices is used to characterise the properties of the neat PU, pure HNT and PU-HNT nanocomposites.

Instrumentation

Morphology of the composites fracture surface was studied using a SEM, Hitachi TM 3000. SEM images have a characteristic 3-D appearance and are therefore useful for judging the surface structure of the sample. Tensile properties were determined using an Instron universal testing machine (INSTRON 5567), with a 200-Newton load transducer, according to the ASTM D-638 type V method standard. The crosshead speed was 50 mm min^{-1} and all tests were performed at room temperature. The three-point bending test (flexural test) was carried out using 100-kN universal testing machine according to specification stated in Instron 8801 (UK). Speed of the test was set at 10 mm min^{-1}. Shape of specimen used for flexural test was tested according to ASTM D790. The Charpy impact strength tests for both un-notched and single-notched specimens at room temperature were carried out using ASTM D5942 equipped with a pendulum impact machine (MT3016, UK). A pendulum with Terco-15 J was selected for the impact tests. Dynamic mechanical measurements (DMA) were determined using Pyris Diamond DMA which consisting of a temperature programmer and controller. Samples with dimensions of 11·0 mm × 20·0 mm × 2·9 mm, prepared by compression press were used for analysis. It measures dynamic modulus, both storage (E') and loss modulus (E''). DMA spectra were taken in tensile mode at 1 Hz frequency in a broad temperature range (50–150°C) with a programmed heating rate of 2°C min^{-1} using dual cantilever method, force applied was 6·35 N, displacement 20 μm. Thermal stability and composition were assessed

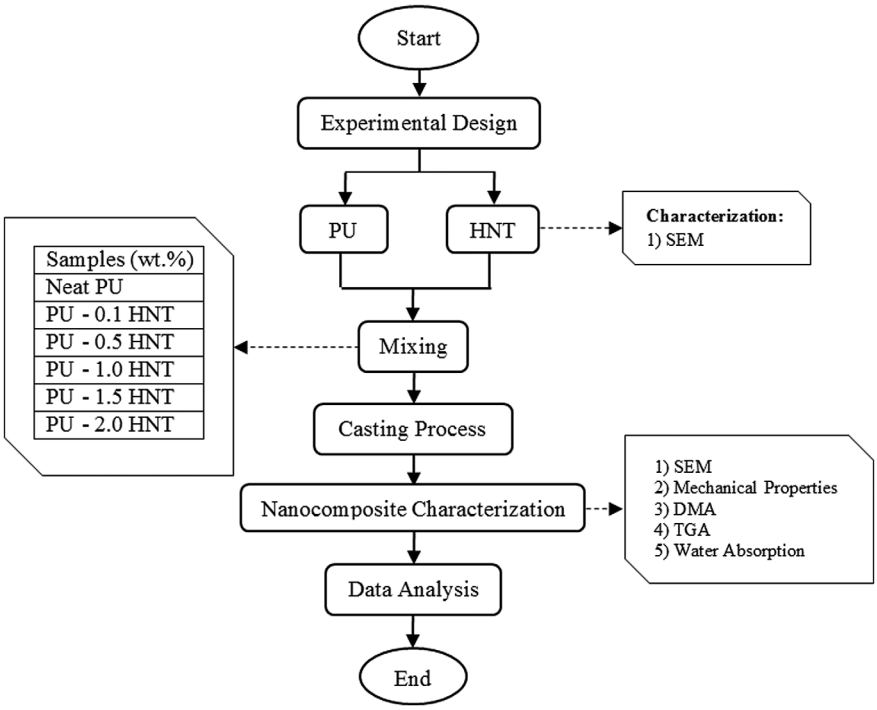

Figure 1. Sample preparation and experimental set-up.

using thermogravimetry (Perkin-Elmer Pyris 1 TGA, 30–1021°C at 10°C·min^{-1} under nitrogen with change to air at 700°C). Samples of about 7–8 mg each were heated from 50 to 950°C at a rate of 10°C min^{-1} under nitrogen atmosphere. Finally, five samples of rectangular shape were used for the measurements of water absorption. Each sample was dried and weighted in air (M_0), then immersed in distilled water, taken out and weighted again (M_1). Water absorption was calculated according to ASTM D 570-81 (ASTM, 2001b) using Equation (1).

$$\text{Water absorption}\,(\%) = \frac{M_1 - M_0}{M_0} \times 100\% \quad (1)$$

Results and discussion

SEM of HNTs and neat PU

SEM image for neat PU and HNT nanoparticles is shown in Figure 2. SEM image of PU, Figure 2(a), surface shows that the surface is smooth with some vacant areas distributed all over the surface with sizes range from 100 to 450μm. SEM image of HNT nanoparticles is shown in Figure 2(b). Based on the estimation included in the legend of the SEM image of HNT, the average length of the HNT tubes is about 200 nm. Within the concept of these numbers, the topic under investigation belongs to the nanotechnology.

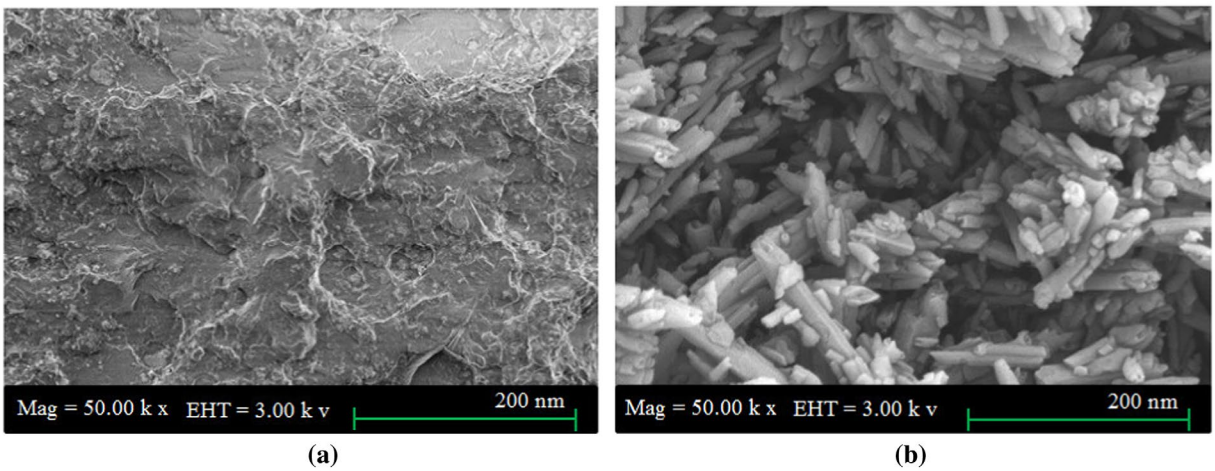

Figure 2. SEM microphotographs for (a) PU and (b) HNT.

SEM for tensile- and impact-fractured surface of PU-HNTs

The fracture is defined as the separation of two parts from each other under the influence of force which is known in the engineering field as stress. As the two parts are separated, the molecules are displaced further from each other. If the displacement is perpendicular to the surface, the fracture is called tensile fracture. For impact fracture, the displacement is not perpendicular to the fractured surfaces.

The SEM images of the tensile-fractured surface of PU-HNT nanocomposites at different HNT loadings are shown in Figure 3 (a)–(e). The fractured surfaces show the presence of HNT represented by white dots distributed over the PU surface. As the HNT percentage loading increases, the density of the white dots and their relevant sizes increase. The increase in the size suggests the occurrence of agglomeration which has significant effect on the physio-mechanical properties of the composites. The fractured tensile surface at 0·1 and 0·5 wt.% HNT do not show clear cracks in the fractured surface as shown in Figure 3(a) and (b). The crack in the surface becomes very clear as the HNT loading increases from 1·0 to 2·0 wt.% HNT

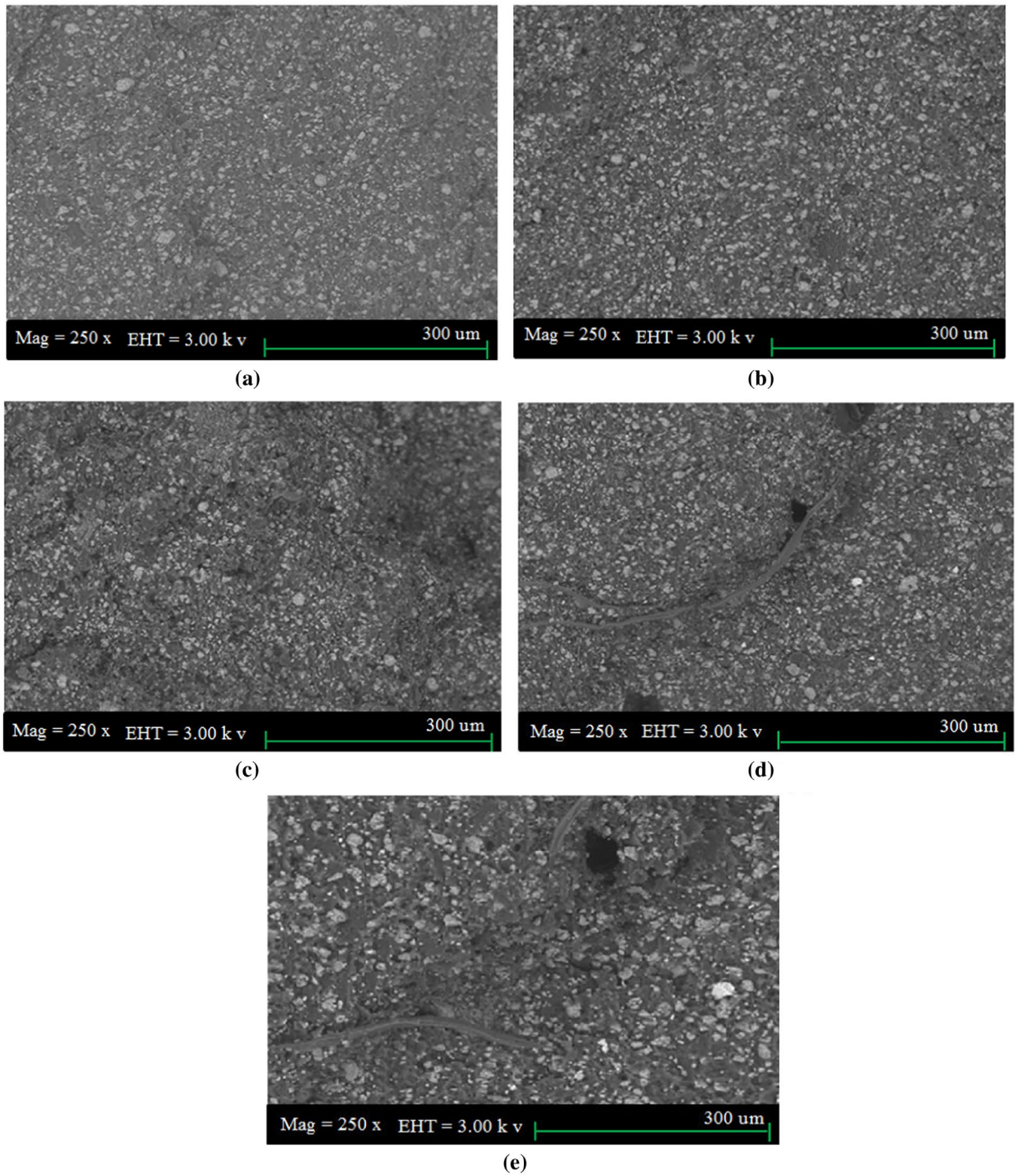

Figure 3. SEM images of tensile fracture of PU-HNT for (a) PU-0·1 wt.% HNT, (b) PU-0·5 wt.% HNT, (c) PU-1·0 wt.% HNT, (d) PU-1·5 wt.% HNT and (e) PU-2·0 wt.% HNT.

as shown in Figure 3 (c)–(e). SEM images shown in Figure 3 suggest that the tensile strength increases and then decreases due to the formation of the cracks where a certain dependency could be drawn between the tensile strength and the agglomeration of HNT in PU-HNT matrix.

The SEM images of the impact-fractured surface of PU-HNT nanocomposites at different HNT loadings are shown in Figure 4 (a)–(e). The similarity of the SEM images of the impact-fractured surface and the tensile-fractured surface is characterised by the distribution of HNT nanoparticles over PU surface and the formation of agglomerated HNT nanoparticles. However, SEM images of the impact-fractured surfaces do not show the presence of cracks possibly because of the sudden cut of the surface rather than slow cutting in case of the tensile fracture. SEM images are, again, support that the mechanical properties improve until the agglomeration of HNT nanoparticles starts forming on PU-HNT matrix.

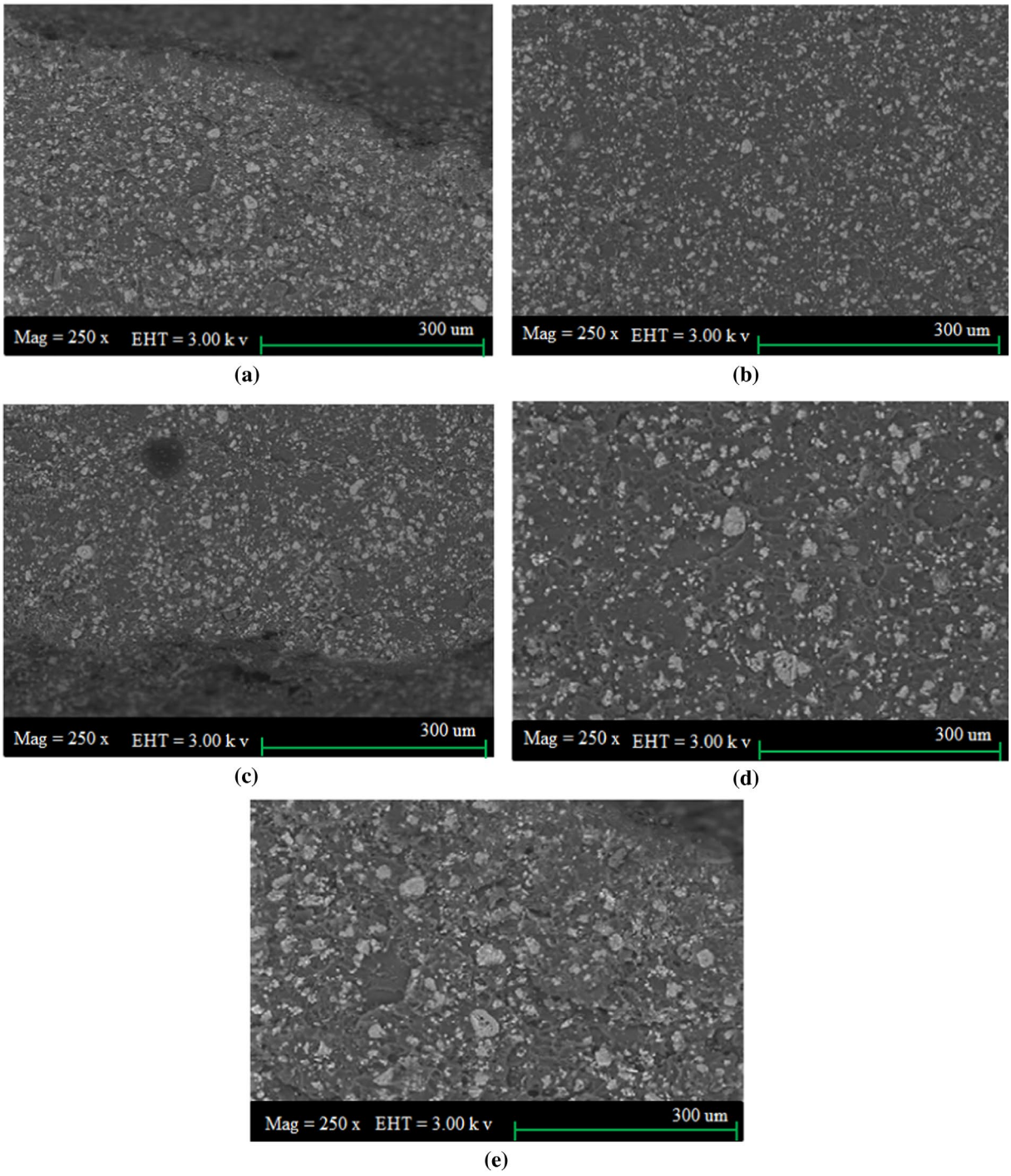

Figure 4. SEM images of impact fracture of PU-HNT for (a) PU-0·1 wt.% HNT, (b) PU-0·5 wt.% HNT, (c) PU-1·0 wt.% HNT, (d) PU-1·5 wt.% HNT and (e) PU-2·0 wt.% HNT.

Tensile test

The tensile strength which measures the capacity of a material to withstand loads tending to elongate achieving the ultimate tensile strength which represents the maximum strength before breaking that material. The results of the tensile strength of neat PU, PU-0·1 wt.% HNT, PU-0·5 wt.% HNT, PU-1·0 wt.% HNT, PU-1·5 wt.% HNT and PU-2·0 wt.% HNT are shown in Figure 5. The thermostat neat PU exhibits tensile strength of 8·19 MPa. As the HNT filler increases from 0·1 to 1·0 wt.%, the tensile strength increases attaining the maximum value of 11·72 MPa by showing a significant percentage increase of about 43%. Then the tensile strength decreases as the HNT amount increases to 2·0 wt.% at which the tensile strength inclined to reach 8·98 MPa. The behaviour of PU-HNT nanocomposite could be understood based on the versatile behaviour of PU which has the ability to change due to external parameters such as temperature, pressure and recently adding small quantities of nanomaterials. PU attains its highest rigidity when a 1·0 wt.% HNT is added, and, again, it loses it rigidity and become plastic/rubber like as the HNT% increases.[38] Based on SEM images shown in Figures 3 and 4, the formation of the agglomerated HNTs nanoparticles has adversely affected the improvement in the mechanical properties caused by the presence of HNT nanoparticles. This behaviour of attaining maximum tensile strength followed by a reduction at certain HNT loading percentage and its relation with agglomeration of HNT nanoparticles as seen in SEM images could further explain the similar behaviour of PU-HNT nanocomposites for other mechanical properties as they were presented in the following discussion.

The Young modulus was then tested for neat PU and PU-different percentages HNT as fillers as presented in Figure 6. Young modulus is the measure of elasticity of the material which could reach infinity for perfectly rigid material. The PU-HNT nanocomposite reaches its highest rigidity of 1407·25 MPa or becomes very stiff when the HNT added to PU at 1·0 wt.%. On both sides of 1 wt.% HNT, PU-HNT nanocomposite shows less rigidity and better elasticity. The nano-sized HNT fillers were bonded to the polyurethane molecular chain so that the mobility of the molecules was restricted.[39] Therefore, the flexibility reduces and stiffness increases. Ismail et al. [40], also found that there was increase in the Young's modulus after 0·5 wt.% of filler loading in the polymer matrix.

The maximum load that PU and PU-HNT nanocomposite can hold before breaking down, which takes place beyond the yield, is shown in Figure 7. This type of measurements is related, to a certain extent, to the elasticity and brittleness of the sample under test. The PU-1·0 wt.% HNT nanocomposite can hold the maximum load of 353·26 N. Other samples including neat PU show less maximum load except the PU-1·0 wt.% HNT which shows almost same maximum load as PU-0·5 wt.% HNT. Based on the results presented in Figure 7, loading HNT to PU has improved the maximum load by about 43% which is same improvement of the tensile strength discussed earlier. The results also show that the loading up to 2·0 wt.% HNT was not enough to bring the PU-HNT nanocomposite to the original status regarding the maximum load by showing an improvement of about 10%. The findings here support the findings of the tensile strength shown in Figure 5.

The elongation at break measurements is another avenue to look at the elasticity–brittleness behaviour of the neat PU along with PU-HNT nanocomposite as shown in Figure 8. The neat PU sample has shown 5% elongation at break which suggests that neat PU is not completely rigid rather than it has a mixture of rigidity and elasticity with dominant rigidity. The rigidity decreases as the HNT filler is loaded to PU as shown in Figure 8. At PU 1·0 wt.% HNT nanocomposite, the sample can be elongated to 20% of its original length before breaking down. The overall loading HNT to PU increases the elongation percentage to finally reach 75% of the original sample length before breaking down. These findings have a significant importance for choosing suitable application for PU-HNT nanocomposite in industry. It is instead of focusing on the durability of the nanocomposite only; the other applications could be beneficial such as using this nanocomposite for packaging or similar applications.

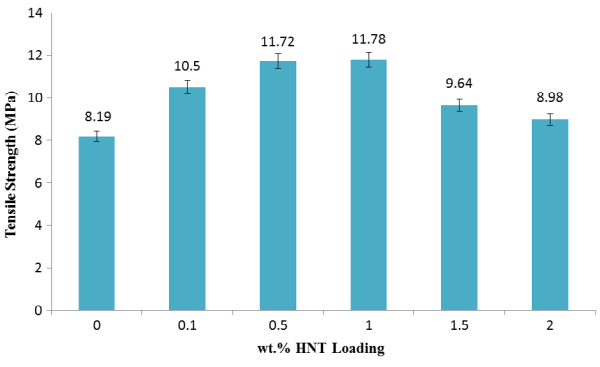

Figure 5. Tensile strength of the PU-HNT nanocomposite.

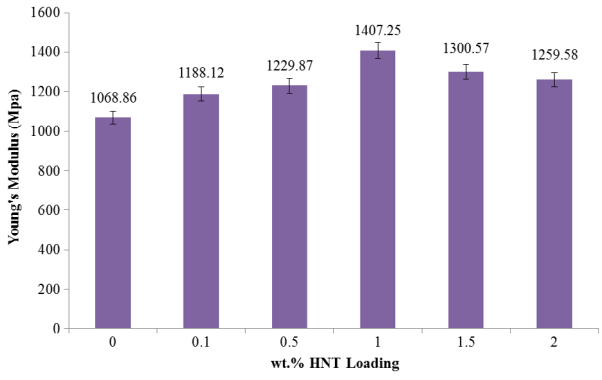

Figure 6. Young's modulus of the PU-HNT nanocomposite.

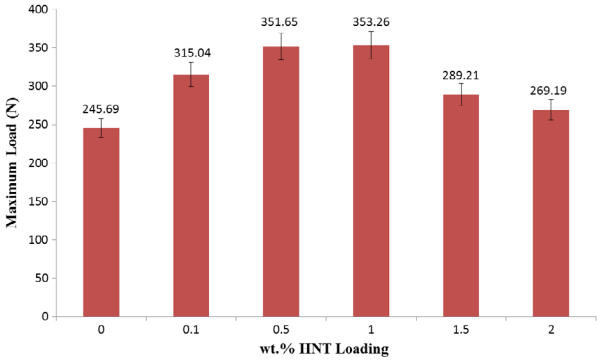

Figure 7. Maximum load of the PU-HNT nanocomposite.

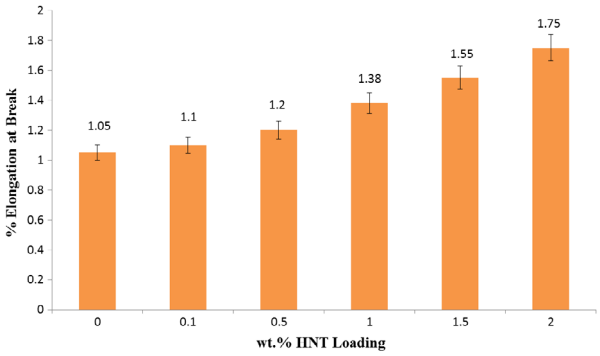

Figure 8. Elongation at break of the PU-HNT nanocomposite.

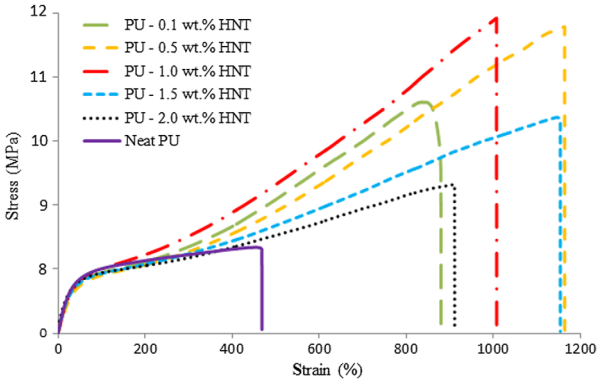

Figure 9. Stress–strain curves of PU-HNT nanocomposite.

Finally, the stress–strain relationship for the samples containing 0, 0·1, 0·5, 1·0, 1·5 and 2·0 wt.% HNT nanocomposite are presented in Figure 9. The stress–strain curves provide very important information regarding the Young's modulus determination and the yield. The curves shown in Figure 9 exhibit a non-monotonic mechanical properties' trend.

Flexural test

Flexural strength (modulus of rupture or fracture strength) is a property of a material that defines the highest stress experienced within the material at the moment of rupture. The flexural test requires applying a load at the middle of the sample structure which causes a range of stresses across the depth of the sample. The sample at the middle where the load is applied, exhibits maximum compressive stress, while it shows maximum tensile values at the supporting points. The basic requirement of a successful flexural test is that the sample has to withstand maximum tensile strength before failing under compressive strength; otherwise there is no reason to conduct the flexural test. The flexural test of the neat PU and PU-HNT nanocomposite at different loading is shown in Figure 10. The neat PU shows that the flexural test was successfully conducted up to 65·82 MPa compressive stress.[41] The maximum compressive stress that the nanocomposite can hold appears at 1·0 wt.% HNT where the stress shows 128·15 MPa. This result is in agreement with other results discussed earlier. The compressive stress increased by about 94% and the sample of maximum 2·0 wt.% HNT load shows an increase by 61%.[42]

The maximum load at yield of the neat PU and PU-HNT nanocomposite is shown in Figure 11. The maximum yield is defined as the stress where the material begins to deform plastically. Basically, this test closely related to the elasticity of the material rather than taking the rigidity into account. The maximum load test is also used by engineers to determine the limits of the performance for mechanical components before partial or total deformation could occur. The maximum load at yield tests help in reshaping the material or explore the limitations to separate the material by cutting or shearing. The neat PU sample shows that a load of 39·49 N is enough to deform it, while the PU-1·0 wt.% HNT needs 76·89 N to achieve same level of deformation. Based on this result, the PU-HNT at 1·0 wt.% loading shows an increase of 94% which agrees with the result obtained for the flexural test. The overall results of the maximum load at the yield show clearly that the PU sample is vulnerable to any outside influence such as pressure or loading. The result also shows that even at loading of 2·0 wt.% of HNT, PU-HNT nanocomposite still shows very good elasticity as a loading at the yield shows an increase of about 73% improvement compared to the neat PU.[43]

The deflection is another measurement which shows the transverse behaviour of a material under certain load and can be expressed by angle or distance. The normal and very famous method used to calculate the deflection is the Euler–Bernoulli beam equation. The homogeneity of the material is very essential property to obtain a very reliable result and this is the reason a morphological test should be taken to show the dispersion of HNT in PU. Another important condition is the length to high ratio (called sometimes as aspect ratio or slender) which has to be greater than 10 – the condition that is satisfied in this work based on preparation of the samples. Figure 12 shows the deflection caused by a certain load of the neat PU and PU-HNT nanocomposites as shown in the figure. The neat PU can sustain deflection up to only 14·32 mm. As the HNT percentage loading to PU, the

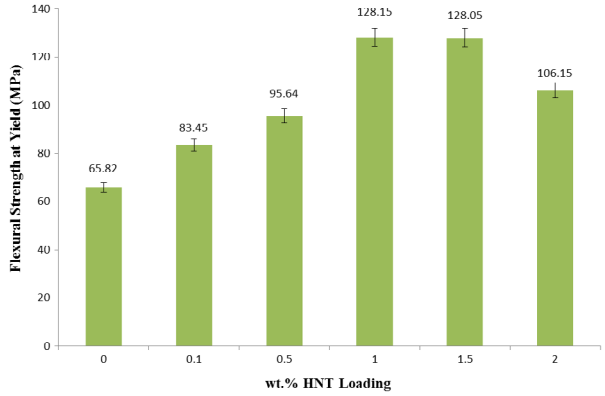

Figure 10. Flexural strength at yield of the PU-HNT nanocomposite.

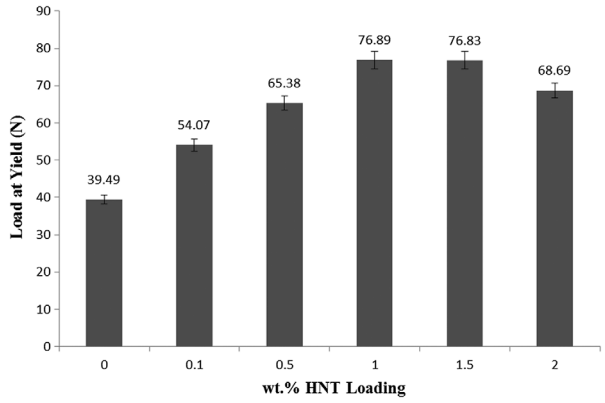

Figure 11. Load at yield of the PU-HNT nanocomposite.

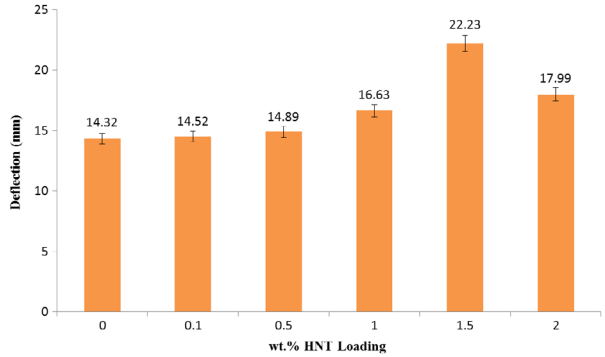

Figure12. Deflection of the PU-HNT nanocomposite.

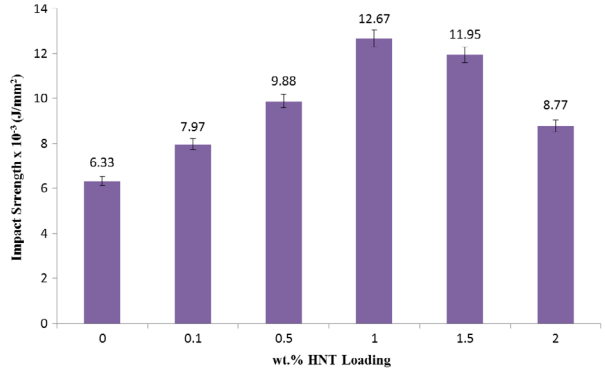

Figure13. Impact strength of the PU-HNT nanocomposite for un-notched specimens.

deflection increases showing better elasticity until HNT of 1·5 wt.% where the sample shows 22·23 mm. The result here is diverted from other consistent result that PU-1·0 wt.% HNT is the maximum or the critical property as shown in all mechanical measurements discussed earlier. The diversion of the deflection measurement could be attributed to either an experimental error or, more likely, to very similar results between the 1·0 and 1·5 wt.% HNT in previous results. The improvement of the elasticity based on the neat PU is about 55%, while the maximum loading of 2·0 wt.% HNT shows only 25% improvement. In the shadow of the results here and other mechanical measurements, it is important to add at least one test between 1·5 and 2·0 wt.% HNT to better localise the critical values of the mechanical properties.

Impact test

The impact test is usually carried out to show how a material in a rod or a plate form withstands as a sudden perpendicular applied load. The impact test is expressed by the energy or, more specifically, the intensity which is energy per are time per surface area. The basic condition for the impact test is to fracture the specimen by evenly distributing very big load throughout the sample. There are two impact tests one without notch and the other with a notch where the notch is a groove made by very sharp razor which is equipped with the instrument and determined by a standard based on the machine itself.

The impact strength test of un-notched PU and PU-HNT nanocomposites samples are carried out and the results are shown in Figure 13. The impact strength of the neat PU is measured at $6{\cdot}33 \times 10^{-3}$ J mm^{-2} and as HNT loading increases, the impact factor increases showing its maximum at $12{\cdot}67 \times 10^{-3}$ J mm^{-2} at 1·0 wt.% HNT loading. The results shows an improvement of about 100% compared to the neat PU which, by increasing HNT loading, declines to only 38% at the highest HNT loading of 2 wt.%. Seemingly, the morphology of the higher HNT loading samples becomes distorted as suggested by SEM analysis.

The last mechanical test is shown in Figure 14 through which same impact test was repeated with only one

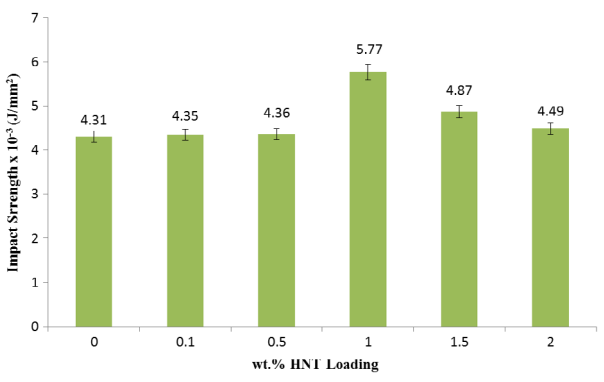

Figure 14. Impact strength of the PU-HNT nanocomposite for single-notched specimens.

difference by making a notch on the sample surface. As expected, the neat PU sample shows less impact strength test at $4{\cdot}31 \times 10^{-3}$ J mm^{-2} by declining 32% based on the original un-notched sample. The impact strength increases as HNT loading percentage increases for the nanocomposites samples and reaches its maximum at $5{\cdot}77 \times 10^{-3}$ J mm^{-2} and, similarly, to un-notched samples, declines for higher HNT loading contents.

The effect of notching the sample could be used to show how the smoothness of the sample surfaces plays an important role in the impact strength.[44] The results show that the maximum impact strength – both occurs at HNT of 1·0 wt.% loading – declines by a significant amount of 120%. This decrease is marked in science and engineering as a phenomena that deserved to be highlighted and studied thoroughly.

Dynamic Mechanical analysis (DMA)

Polymers combine the properties of solid elasticity and the Newtonian fluidity. The solid property is characterised by deformation which is caused by stress, while the strain is the relevant response. The DMA technique provides viscoelastic measurements response of a material under the influence of a sinusoidal oscillation force which might be in the form of a strain (strain-controlled instrument) or a stress (stress-controlled instrument). The stress/strain could be in any mechanical form such as tension, compression or torsion. For a perfectly elastic solid, the strain and the stress are in phase, while in a purely viscous media, the strain lags the stress by 90°. The phase difference lies somewhere between 0 and 90° for all other solid materials depending on the rigidity

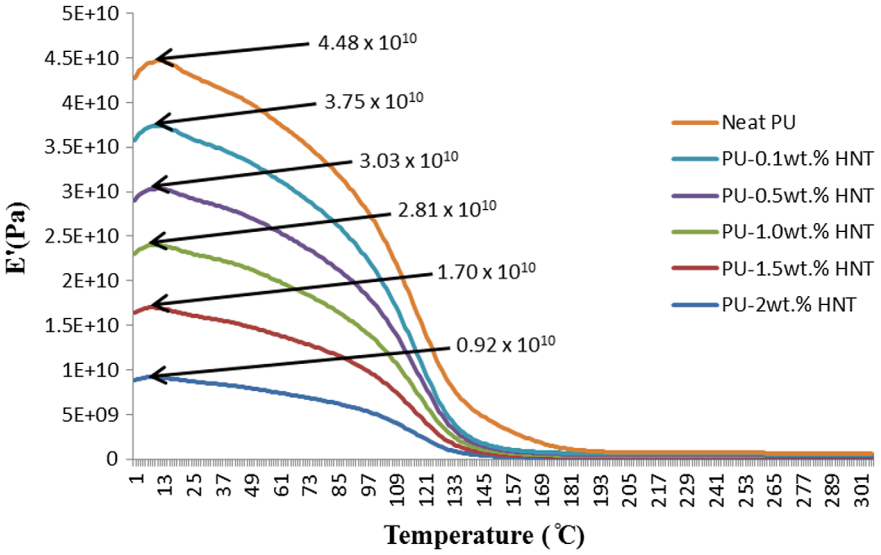

Figure 15. Storage modulus of PU-HNT nanocomposite.

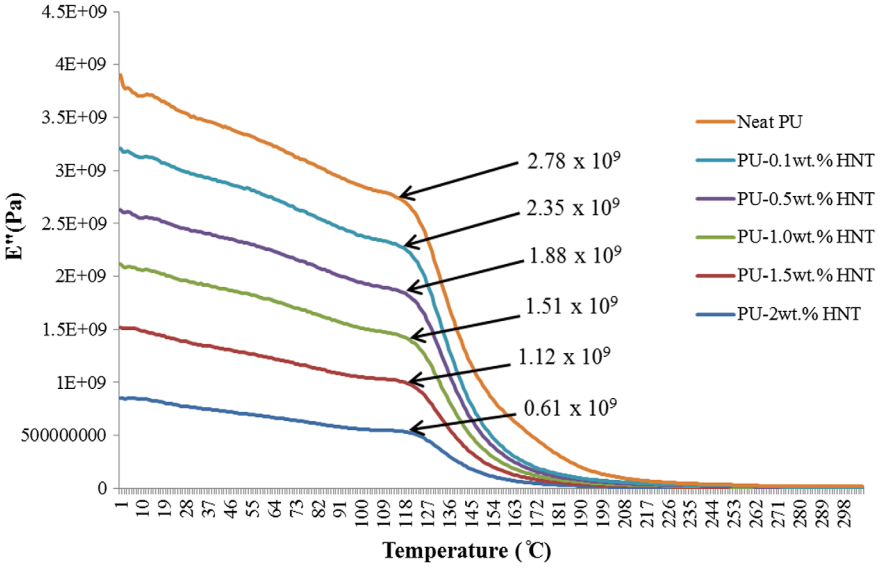

Figure 16. Loss modulus of PU-HNT nanocomposite.

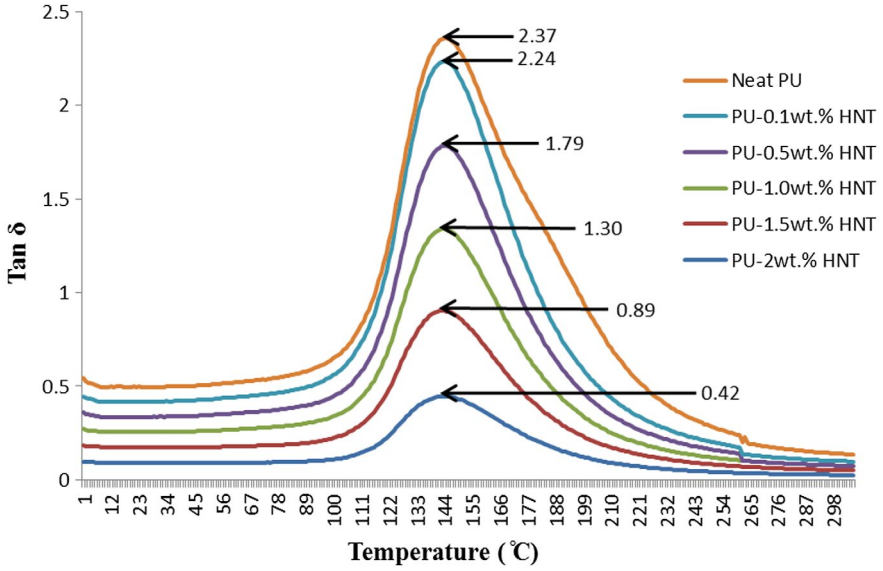

Figure 17. Loss tangent of PU-HNT nanocomposite.

and elasticity. The storage modulus (E') measures the stored energy, while the loss modulus (E'') represents the dissipated energy as heat, for example. The DMA technique is used to identify the mechanical properties of a material in terms of temperature or strain rate (frequency). The region of the linear viscoelastic region is used for DMA tests because in this region the modulus is independent of the applied stress or strain magnitude. Generally, the DMA characterises the glass transition (T_g) temperatures, storage and loss moduli and heat deflection or softening points.

Figure 15 shows the storage modulus of neat PU and PU-HNT nanocomposites as a function of temperature. All materials show maximum storage ability at about 13°C after which the storage modulus is fading out exponentially. The results in Figure 15 suggest that the neat PU has the best storage modulus ability which decreases as HNT content increases from 0·1 to 2·0 wt.%. The results also show that the highest temperature at which E can be tested for neat PU appears at about 180°C or lower, while the maximum temperature of PU-2·0 wt.% HNT is shifted to a lower temperature of 137°C.

The loss modulus (E'') curves obtained from DMA instrument for neat PU and PU-HNT nanocomposite are shown in Figure 16. The loss modulus curves showed that neat PU crystallises at 126°C, while PU with addition of 0·1 wt.% of HNT occurs at 129·12°C. This is indicative that adding a small amount of HNT could shift the crystallisation temperature (T_c) of PU. The addition of PU-HNT into PU matrix enhances the nucleation process on PU crystallisation. High surface area of the PU-HNT provides nucleation sites for the PU to crystallise.

Figure 17 shows the loss tangent (tan δ), which is defined as the ratio of (E'/E'') of neat PU or PU-HNT nanocomposite. The loss tangent is used to measure the melting temperature (T_m). The results show that T_m shifts from 147 to 142°C for PU-2·0 wt.% HNT.

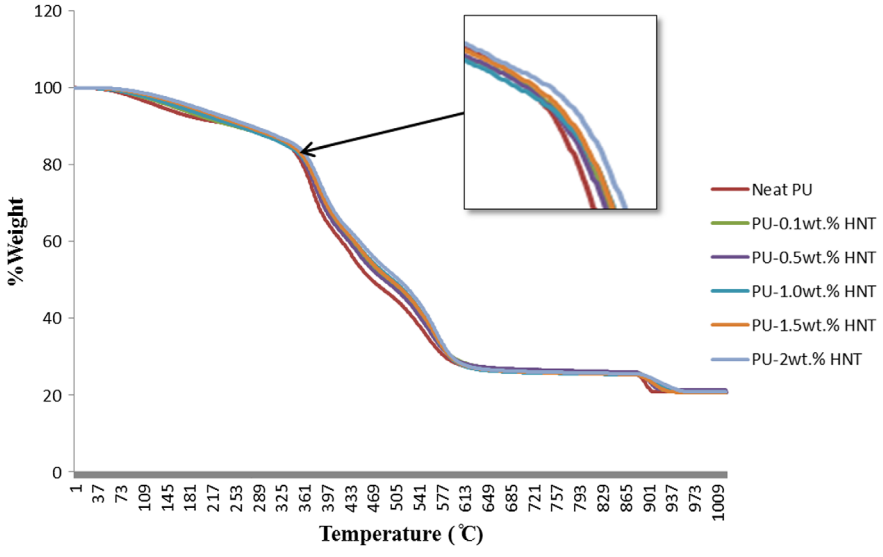

Figure 18. Thermogravimetric analysis of PU-HNT nanocomposite.

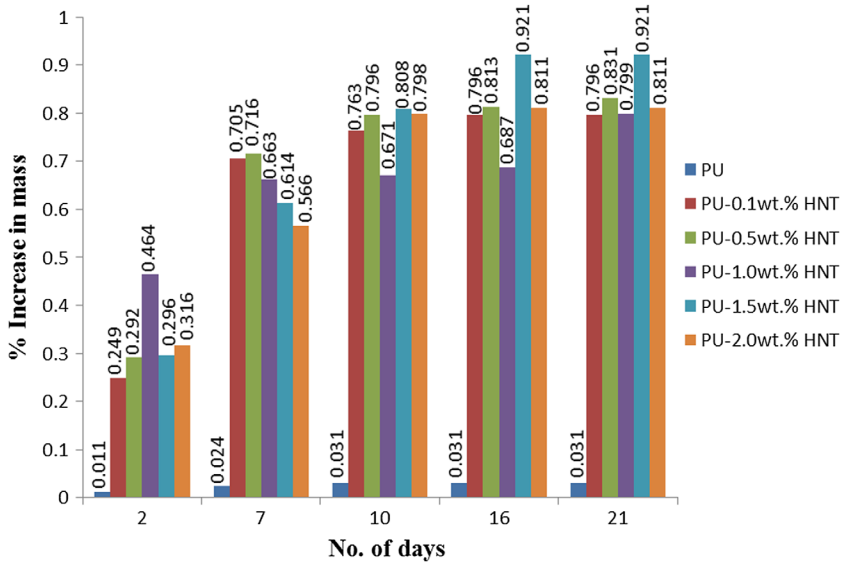

Figure 19. % Increase in mass of the PU-HNT nanocomposite.

Thermogravimetric analysis (TGA)

The TGA curves for neat PU and PU-HNT nanocomposite at different loading are shown in Figure 18. For the PU-HNT, the whole degradation steps can be observed from about 30 to 989°C. Generally, the weight loss of various loading of PU-HNT nanocomposite does not show a significant difference suggesting that adding small HNT quantities to PU has almost no serious influence on the water contained in the matrix. The results in Figure 18 show four major regions of the weight loss: between 30 and 343°C, between 343 and 585°C, between 585 and 881°C and, finally, between 881 and 989°C. The rate of the weight loss in these four regions is: 5·7, 19·0, 0 and 8·3%, respectively. The highest weight loss rate appears in the second region of 343 and 585°C. The results also show that there is no weigh loss between 585 and 881°C. Overall, the PU-HNT nanocomposite up to 2·0 wt.% HNT do not show a significant difference which suggests that the elasticity gained for the nanocomposite has almost no effect on the water contained in the matrix.

Water absorption

The tendency of neat PU and PU-HNT nanocomposites to absorb water is examined. All samples were dried and weighed in air, and then they are immersed (soaked) in distilled water for 21 days at room temperature. The weight of each sample was taken after 2, 7, 10, 16 and 21 days where after each of these days, the surface of the samples were dried by a piece of cloth and the difference in the weight were recorded as shown in Figure 19. The neat PU sample showed very slight increase in the water content by 0·01, 0·02, 0·03, 0·03 and 0·03, respectively. The results of neat PU show that the absorption of water is very minimal due the natural properties of PU as a water resistant agent. For the PU-HNT nanocomposite samples, the absorption of water shows almost same trend. The potentiality of each sample to absorb water reaches saturation by the 16th day of soaking in water. All PU-HNT nanocomposite samples absorbed water due to the hydrophilic nature of the filler HNT incorporated in –OH group.

Conclusions

Improving the mechanical and thermal properties of PU is very important because the optimising these properties is very crucial to the essential demand for industry and technology. The thermo-mechanical properties are improved by adding HNT nanoparticles to PU at very small percentage amount at 0·1, 0·5, 1·0, 1·5 and 2·0% based on the weight. The effect of loading HNT is very prominent as mechanical and thermal properties are tested using several techniques such SEM, tensile strength, elongation, Young modulus, maximum load at yield, DMA and water resistivity of PU-HNT. SEM images of the fracture surface have shown two features: the formation of agglomerated HNT over the surface and the potentiality of PU-HNT nanocomposites to having cracks at about 1·0% HNT loading. The mechanical properties were improved by 43% for the tensile to about 94% for maximum load at the yield before adversely reduced due to the agglomeration and cracks. Even the mechanical properties declined after 1·0% HNT loading, however, the mechanical properties never return the PU-HNT nanocomposite to the standard of PU alone. The effect of cracks, which has naturally happened, a test was performed to see the effect of creating notched on the PU-HNT surface. The result has shown a significant effect of such artificial crack by reducing impact strength by 120% compared with non-notches sample. This result shows the importance of the smoothness of the surface as well as preventing the formation of cracks.

DMA analyses of storage and loss modulus, which have tremendous applications in industry, have shown that the crystalline temperature and melting temperature were affected – the results that lead to expand the use of PU-HNT nanocomposite. The water solubility and water resistivity are the last two tested properties that suggest both PU and PU-HNT are still resistive to water – the phenomena that could help in determining the scope of using PU and PU-HNT nanocomposite.

Author contributions

T. S. G. has written the manuscript. A. B. S., M. N. A. and A. A. H. K. have supervised the whole work. A. A. A. A. was the principle investigator and wrote the manuscript.

Acknowledgements

The authors thank Universiti Kebangsaan Malaysia and the Ministry of Higher Education for the grants and financial support AP-2013-10 and FRGS/2/2013/TK01/UKM/02/3 to support his work.

Disclosure statement

No potential conflict of interest was reported by the authors.

Funding

This work was financially supported by Universiti Kebangsaan Malaysia [grant number AP-2013-10]; the Ministry of Higher Education [grant number FRGS/2/2013/TK01/UKM/02/3].

ORCID

A. A. Al-Amiery http://orcid.org/0000-0003-1033-4904

References

[1] Szycher M. Szycher's handbook of polyurethanes. Boca Raton (FL): CRC press; 1999.
[2] Ionescu M. Chemistry and technology of polyols for polyurethanes. Shawbury: iSmithers Rapra Publishing; 2005.
[3] Bothiraja C, Thorat UH, Pawar AP, et al. Chitosan coated layered clay montmorillonite nanocomposites modulate oral delivery of paclitaxel in colonic cancer. Mater Technol. 2014;29(sup3):B120–B126.
[4] Farrugia BL, Simmons A, Jasieniak M, et al. Platelet interactions with polyurethane nanocomposites: effect of organic modifier terminal functionality. Mater Technol. 2014;29(sup3):B114–B119.
[5] Kim BS, Kim BK. Enhancement of hydrolytic stability and adhesion of waterborne polyurethanes. J Appl Polym Sci. 2005;97:1961–1969.
[6] Lu Y, Tighzert L, Dole P, et al. Preparation and properties of starch thermoplastics modified with waterborne polyurethane from renewable resources. Polymer. 2005;46:9863–9870.
[7] Lu Y, Tighzert L, Berzin F, et al. Innovative plasticized starch films modified with waterborne polyurethane from renewable resources. Carbohydr Polym. 2005;61:174–182.
[8] Shchukin DG, Sukhorukov GB, Price RR, et al. Halloysite nanotubes as biomimetic nanoreactors. Small. 2005;1:510–513.
[9] Noro H. Hexagonal platy halloysite in an altered tuff bed, Komaki city, Aichi prefecture, *Central Japan*. Clay Miner. 1986;21:401–415.
[10] Azam MA, Nawi ZM, Azren NM, et al. Synthesis of Fe catalyst nanoparticles by solution process towards carbon nanotube growth. Mater Technol. 2015;30(sup1):A8–A13.
[11] Antill SJ. Halloysite: a low-cost alternative. Aust J Chem. 2003;56:723–723.
[12] Du M, Guo B, Jia D. Thermal stability and flame retardant effects of halloysite nanotubes on poly (propylene). Eur Polym J. 2006;42:1362–1369.
[13] Wang H, Sun J, Li J, et al. Roughness modelling analysis for milling of carbon fibre reinforced polymer composites. Mater Technol Adv Funct Mater. 2015;30:A46–A50.
[14] Liu M, Guo B, Du M, et al. Properties of halloysite nanotube–epoxy resin hybrids and the interfacial reactions in the systems. Nanotechnology. 2007;18:455703.
[15] Du M, Guo B, Liu M, et al. Preparation and characterization of polypropylene grafted halloysite and their compatibility effect to polypropylene/halloysite composite. Polym J. 2006;38:1198–1204.
[16] Du M, Guo B, Lei Y, et al. Carboxylated butadiene–styrene rubber/halloysite nanotube nanocomposites: interfacial interaction and performance. Polymer. 2008;49:4871–4876.
[17] Cypes SH, Saltzman WM, Giannelis EP. Organosilicate-polymer drug delivery systems: controlled release and enhanced mechanical properties. J Controlled Release. 2003;90:163–169.
[18] Cho J, Paul D. Nylon 6 nanocomposites by melt compounding. Polymer. 2001;42:1083–1094.
[19] Zhu J, Uhl FM, Morgan AB, et al. Studies on the mechanism by which the formation of nanocomposites enhances thermal stability. Chem Mater. 2001;13:4649–4654.
[20] Xie W, Xie R, Pan W, et al. Thermal stability of quaternary phosphonium modified montmorillonites. Chem Mater. 2002;14:4837–4845.
[21] Gorrasi G, Tortora M, Vittoria V, et al. Vapor barrier properties of polycaprolactone montmorillonite nanocomposites: effect of clay dispersion. Polymer. 2003;44:2271–2279.
[22] Fredrickson GH, Bicerano J. Barrier properties of oriented disk composites. J Chem Phys. 1999;110:2181–2188.
[23] Vaia RA, Giannelis EP. Polymer melt intercalation in organically-modified layered silicates: model predictions and experiment. Macromolecules. 1997;30:8000–8009.
[24] Krishnamoorti R, Vaia RA, Giannelis EP. Structure and dynamics of polymer-layered silicate nanocomposites. Chem Mater. 1996;8:1728–1734.
[25] Challa V, Nune K, Misra R. The impact of molecular weight on nanoscale supramolecular structure of semiconducting poly (3-hexylthiophene) on carbon nanotubes and photophysical properties. Mater Technol. 2016;31:477–481.

[26] Zhao P, Li S, Gao G, et al. Mechanical behavior of carbon nanotube-reinforced Mg–Cu–Gd–Ag bulk metallic glasses. Mater Sci Eng: A. 2015;641:116–122.
[27] Challa V, Misra R. The periodic crystallisation of polymers on carbon nanotubes: geometrical confinement versus epitaxy. Mater Technol. 2016:1–7.
[28] Gangadoo S, Chapman J. Emerging biomaterials and strategies for medical applications: a review. Mater Technol. 2015;30(sup5):B3–B7.
[29] Gao F. Advances in polymer nanocomposites: types and applications. Sawston: Elsevier; 2012.
[30] Chang PR, Xie Y, Wu D, et al. Amylose wrapped halloysite nanotubes. Carbohydr Polym. 2011;84: 1426–1429.
[31] Gaaz TS, Sulong AB, Akhtar MN, et al. Properties and applications of polyvinyl alcohol, halloysite nanotubes and their nanocomposites. Molecules. 2015;20: 22833–22847.
[32] Mohammad G, Mohammed W, Marzoog TR, et al. Green synthesis, antimicrobial and cytotoxic effects of silver nanoparticles using *Eucalyptus chapmaniana* leaves extract. Asian Pac J Trop Biomed. 2013;3:58–63.
[33] Gaaz TS, Sulong A, Kadhum A, et al. Impact of sulfuric acid treatment of halloysite on physico-chemic property modification. Materials. 2016;9:620.
[34] Wasmi W, Al-Amiery A, Kadhum A, et al. Synthesis of vanadium pentoxide nanoparticles as catalysts for the ozonation of palm oil. Ozone Sci Eng. 2016;38:36–41.
[35] Obayes H, Al-Gebori A, Khazaal S, et al. Hypothetical design of carbon nanotube materials based on [8] circulene. J Nanoelectron Optoelectron. 2015;10:711–716.
[36] Obayes H, Al-Amiery A, Jaffar H, et al. Theoretical study for the preparation of sub-carbon nano tubes from the cyclic polymerization reaction of two molecules from corannulene, coronene and circulene aromatic compounds. J Comput Theor Nanosci. 2013;10:2453–2457.
[37] Wasmi W, Al-Amiery A, Kadhum A, et al. Novel approach: tungsten oxide nanoparticle as a catalyst for malonic acid ester synthesis via ozonolysis. J Nanomater. 2014;2014:1–7.
[38] Lecouvet B, Sclavons M, Bourbigot S, et al. Water-assisted extrusion as a novel processing route to prepare polypropylene/halloysite nanotube nanocomposites: structure and properties. Polymer. 2011;52:4284–4295.
[39] Njuguna J, Pielichowski K, Desai S. Nanofiller-reinforced polymer nanocomposites. Polym Adv Technol. 2008;19:947–959.
[40] Ismail H, Pasbakhsh P, Ahmad Fauzi MN, et al. Morphological, thermal and tensile properties of halloysite nanotubes filled ethylene propylene diene monomer (EPDM) nanocomposites. Polym Test. 2008;27:841–850.
[41] Mahfuz H, Islam MS, Rangari VK, et al. Response of sandwich composites with nanophased cores under flexural loading. Composites Part B. 2004;35:543–550.
[42] Deng S, Zhang J, Ye L, et al. Toughening epoxies with halloysite nanotubes. Polymer. 2008;49:5119–5127.
[43] Fernández-d'Arlas B, Khan U, Rueda L, et al. Study of the mechanical, electrical and morphological properties of PU/MWCNT composites obtained by two different processing routes. Compos Sci Technol. 2012;72: 235–242.
[44] Anderson KS, Hillmyer MA. The influence of block copolymer microstructure on the toughness of compatibilized polylactide/polyethylene blends. Polymer. 2004;45:8809–8823.